Terahertz reflectarray as a polarizing beam splitter

Tiaoming Niu,[1,2,*] **Withawat Withayachumnankul,**[1] **Aditi Upadhyay,**[3] **Philipp Gutruf,**[3] **Derek Abbott,**[1] **Madhu Bhaskaran,**[3] **Sharath Sriram,**[3] **and Christophe Fumeaux**[1]

[1]*School of Electrical & Electronic Engineering, The University of Adelaide, Adelaide, SA 5005, Australia*

[2]*School of Information Science and Engineering, Lanzhou University, Lanzhou 730000, P. R. China*

[3]*Functional Materials and Microsystems Research Group, School of Electrical and Computer Engineering, RMIT University, Melbourne, VIC 3001, Australia*

[*]*niutm@eleceng.adelaide.edu.au*

Abstract: A reflectarray is designed and demonstrated experimentally for polarization-dependent beam splitting at 1 THz. This reflective component is composed of two sets of orthogonal strip dipoles arranged into interlaced triangular lattices over a ground plane. By varying the length and width of the dipoles a polarization-dependent localized phase change is achieved on reflection, allowing periodic subarrays with a desired progressive phase distribution. Both the simulated field distributions and the measurement results from a fabricated sample verify the validity of the proposed concept. The designed terahertz reflectarray can efficiently separate the two polarization components of a normally incident wave towards different predesigned directions of $\pm 30^{\circ}$. Furthermore, the measured radiation patterns show excellent polarization purity, with a cross-polarization level below -27 dB. The designed reflectarray could be applied as a polarizing beam splitter for polarization-sensitive terahertz imaging or for emerging terahertz communications.

OCIS codes: (300.6495) Spectroscopy, terahertz; (230.1360) Beam splitters; (240.6645) Surface differential reflectance; (290.5855) Scattering, polarization.

References and links

1. J. B. Pendry, D. Schurig, and D. R. Smith, "Controlling electromagnetic fields," Science **312**, 1780–1782 (2006).
2. D. Schurig, J. J. Mock, B. J. Justice, S. A. Cummer, J. B. Pendry, A. F. Starr, and D. R. Smith, "Metamaterial electromagnetic cloak at microwave frequencies," Science **314**, 977 (2006).
3. D. Kwon and D. Werner, "Polarization splitter and polarization rotator designs based on transformation optics," Opt. Express **16**, 18731–18738 (2008).
4. J. Valentine, J. Li, T. Zentgraf, G. Bartal, and X. Zhang, "An optical cloak made of dielectrics," Nat. Mater. **8**, 568–571 (2009).
5. H. Chen, C. T. Chan, and P. Sheng, "Transformation optics and metamaterials," Nat. Mater. **9**, 387–396 (2010).
6. N. Yu, P. Genevet, M. A. Kats, F. Aieta, J. Tetienne, F. Capasso, and Z. Gaburro, "Light propagation with phase discontinuities: generalized laws of reflection and refraction," Science **334**, 333–337 (2011).
7. F. Yang, and Z. Mei, T. Jin, and T. Cui, "dc electric invisibility cloak," Phys. Rev. Lett. **109**, 053902 (2012).
8. F. Aieta, P. Genevet, N. Yu, M. A. Kats, Z. Gaburro, and F. Capasso, "Out-of-plane reflection and refraction of light by anisotropic optical antenna metasurfaces with phase discontinuities," Nano Lett. **12**, 1702–1706 (2012).
9. Y. Monnai, K. Altmann, C. Jansen, M. Koch, H. Hillmer and H. Shinoda, "Terahertz beam focusing based on plasmonic waveguide scattering," Appl. Phys. Lett. **101**, 151116 (2012).

#211499 - $15.00 USD Received 8 May 2014; revised 15 Jun 2014; accepted 16 Jun 2014; published 23 Jun 2014

10. N. Grady, J. Heyes, D. Chowdhury, Y. Zeng, M. Reiten, A. Azad, A. Taylor, D. Dalvit, and H. Chen, "Terahertz metamaterials for linear polarization conversion and anomalous refraction," Science **340**, 1304–1307 (2013).
11. C. Tai, S. Chang, and T. Chiu, "Design and analysis of an ultra-compact and ultra-wideband polarization beam splitter based on coupled plasmonic waveguide arrays," IEEE Photon. Technol. Lett. **19**, 1448–1450 (2007).
12. X. Guan, H. Wu, Y. Shi, L. Wosinski, and D. Dai, "Ultracompact and broadband polarization beam splitter utilizing the evanescent coupling between a hybrid plasmonic waveguide and a silicon nanowire," Opt. Lett. **38**, 3005–3008 (2013).
13. K. Yang, X. Long, Y. Huang, and S. Wu, "Design and fabrication of ultra-high precision thin-film polarizing beam splitter," Opt. Commun. **284**, 4650–4653 (2011).
14. M. Rahm, S. Cummer, D. Schurig, J. B. Pendry, and D. R. Smith, "Optical design of reflectionless complex media by finite embedded coordinate transformations," Phys. Rev. Lett. **100**, 063903 (2008).
15. M. Farmahini-Farahani and H. Mosallaei, "Birefringent reflectarray metasurface for beam engineering in infrared," Opt. Lett. **38**, 462–464 (2013).
16. C. Lin, Y. Li, C. Hsieh, R. Pan, and C. Pan, "Manipulating terahertz wave by a magnetically tunable liquid crystal phase grating," Opt. Express **16**, 2995–3001 (2008).
17. C. W. Berry and M. Jarrahi, "Broadband terahertz polarizing beam splitter on a polymer substrate," J. Infrared Milli. Terahz. Waves **33**,127–130 (2012).
18. X. G. Peralta, E. I. Smirnova, A. K. Azad, H. Chen, A. J. Taylor, I. Brener, and J. F. O'Hara, "Metamaterials for THz polarimetric devices," Opt. Express **17**, 773–783 (2009).
19. J. Huang and J. Encinar, Reflectarray Antenna. Wiley Online Library, 2008.
20. A. Tamminen, S. Mäkelä, J. Ala-Laurinaho, J. Häkli, P. Koivisto, P. Rantakari, J. Säily, A. Luukanen, and A. Räisänen, "Reflectarray design for 120-GHz radar application: measurement results," IEEE Trans. Antennas Propag. **61**, 5036–5047 (2013).
21. A. Tamminen, J. Ala-Laurinaho, S. Mäkelä, D. Gomes-Martins, J. Häkli, P. Koivisto, P. Rantakari, J. Säily, R. Tuovinen, A. Luukanen, M. Sipilä, and A. Räisänen, "Near-field measurements of submillimeter-wave reflectarrays," Proc. SPIE **8715**, 871506 (2013).
22. P. Nayeri, M. Liang, R. Sabory García, M. Tuo, F. Yang, M. Gehm, H. Xin, and A. Elsherbeni, "3D printed dielectric reflectarrays: low-cost high-gain antennas at sub-millimeter waves," IEEE Trans. Antennas Propag. **62**, 2000–2008 (2014).
23. T. Niu, W. Withayachumnankul, B. S.-Y. Ung, H. Menekse, M. Bhaskaran, S. Sriram, and C. Fumeaux, "Experimental demonstration of reflectarray antennas at terahertz frequencies," Opt. Express **21**, 2875–2889 (2013).
24. E. Carrasco and J. Perruisseau-Carrier, "Reflectarray antenna at terahertz using graphene," IEEE Antennas Wirel. Propag. Lett. **12**, 253–256 (2013).
25. B. Memarzadeh and H. Mosallaei, "Array of planar plasmonic scatterers functioning as light concentrator," Opt. Lett. **36**, 2569–2571 (2011).
26. A. Pors, M. G. Nielsen, G. D. Valle, M. Willatzen, O. Albrektsen, and S. I. Bozhevolnyi, "Plasmonic metamaterial wave retarders in reflection by orthogonally oriented detuned electrical dipoles," Opt. Lett. **36**, 1626–1628 (2011).
27. L. Zou, W. Withayachumnankul, C. M. Shah, A. Mitchell, M. Bhaskaran, S. Sriram, C. Fumeaux, "Dielectric resonator nanoantennas at visible frequencie," Opt. Express **21**, 1344–1352 (2013).
28. Y. Yifat, M. Eitan, Z. Iluz, Y. Hanein, A. Boag, and J. Scheuer, "Highly efficient and broadband wide-angle holography using patch-dipole nano-antenna reflectarrays," Nano Lett. **14**, 2485–2490 (2014).
29. J. Encinar, L. Datashvili, J. Zornoza, M. Arrebola, M. Sierra-Castañer, J. Besada-Sanmartín, H. Baier, and H. Legay, "Dual-polarization dual-coverage reflectarray for space applications," IEEE Trans. Antennas Propag. **54**, 2827–2837 (2006).
30. J. Perruisseau-Carrier, "Dual-polarized and polarization-flexible reflective cells with dynamic phase control," IEEE Trans. Antennas Propag. **58**, 1494–1502 (2010).
31. D. Pozar and S. Targonski, "A microstrip reflectarray using crossed dipoles," Antennas and Propagation Society International Symposium, 1998. IEEE, 21–26 June, 1008–1011 (1998).
32. L. Li, Q. Chen, Q. Yuan, K. Sawaya, T. Maruyama, T. Furuno, and S. Uebayashi, "Frequency selective reflectarray using crossed-dipole elements with square loops for wireless communication applications," IEEE Trans. Antennas Propag. **59**, 89–99 (2011).
33. T. Niu, W. Withayachumnankul, D. Abbott, and C. Fumeaux, "Design of polarization-dependent reflectarray for terahertz waves," The 2014 International Workshop on Antenna Technology, Sydney, 4–6 March, 210–212 (2014).
34. F. C. E. Tsai and M. E. Bialkowski, "Designing a 161-element Ku-band microstrip reflectarray of variable size patches using an equivalent unit cell waveguide approach," IEEE Trans. Antennas Propag. **51**, 2953–2962 (2003).
35. I. E. Khodasevych, C. M. Shah, S. Sriram, M. Bhaskaran, W. Withayachumnankul, B. S.-Y. Ung, H. Lin, W. S. T. Rowe, D. Abbott, and A. Mitchell, "Elastomeric silicone substrates for terahertz fishnet metamaterials," Appl. Phy. Lett. **100**, 061101 (2012).
36. P. Gutruf, C. Shah, S. Walia, H. Nili, A. Zoolfakar, C. Karnutsch, K. Kalantar-zadeh, S. Sriram and M. Bhaskaran, "Transparent functional oxide stretchable electronics: micro-tectonics enabled high strain electrodes," NPG Asia Materials **5**, e62 (2013).

#211499 - $15.00 USD Received 8 May 2014; revised 15 Jun 2014; accepted 16 Jun 2014; published 23 Jun 2014

37. E. Almajali, D. A. McNamara, J. Shaker, and M. Chaharmir, "Feed image lobes in offset-fed reflectarrays: diagnosis and solution," IEEE Trans. Antennas Propag. **62**, 216–227 (2014).
38. S. D. Targonski and D. M. Pozar, "Minimization of beam squint in microstrip reflectarrays using an offset feed," IEEE Antennas and Propagation Society International Symposium, MD, 21–26 July, 1326–1329 (1996).
39. J. A. Encinar, "Design of two-layer printed reflectarrays using patches of variable size," IEEE Trans. Antennas Propag. **49**, 1403–1410 (2001).

1. Introduction

For centuries, controlling the propagation of electromagnetic waves has been one of the intensively researched topics in science and engineering. From conventional optical lenses to the exotic artificially patterned structures of today, scientists and engineers have progressively introduced more degrees of freedom in both theoretical and experimental aspects of beam manipulation for increasingly sophisticated applications [1–10]. Beam splitters with polarization-dependent properties can play an important role in applications requiring high polarization purity or polarization-dependent multiplexing/demultiplexing. In the optical range, coupled plasmonic waveguide arrays [11], an asymmetrical directional coupler [12], and a 34-layer polymer thin-film [13] have been proposed for polarizing beam splitters. Further concepts inspired by metamaterials have been introduced for designing or realizing beam splitters across different spectral ranges [14, 15].

In the terahertz regime, due to lack of suitable naturally birefringent materials and because of high intrinsic material loss, devices that can separate the incident waves with polarization-dependent properties still remain challenging to realize. Implementations include a magnetically tunable liquid crystal phase grating used for tuning the ratio of the zeroth and first-order diffracted terahertz waves [16]. This fabricated terahertz beam splitter achieved modest efficiency of around 40%, although it was shown to provide high extinction ratio and tunability across a wide frequency range. To improve the efficiency, Berry *et. al*. [17] demonstrated the potential of a subwavelength silver grating fabricated on a high-density polymer substrate for constructing a terahertz polarizing beam splitter in a wide frequency band. In [18], a metamaterial structure based on circular split rings was used to control the characteristics of transmitted terahertz waves, with effects strongly dependent on the incident polarization. One aspect worthy to mention here is that these designs mainly focus on polarization beam-splitting in transmission, with emphasis on frequency tunability. Beam splitting operation in reflection mode remains to the best of our knowledge relatively unexplored.

One feasible pathway for beam splitting in reflection is offered by the concept of reflectarrays. Owing to their high efficiency and flat profile, reflectarrays have been adopted widely in the microwave and millimeter-wave regions [19–21], and implementations have been extended across the electromagnetic spectrum to the terahertz [22–24] and optical regimes [25–28] with various functionalities such as beam deflection, focussing and beam shaping. Among the versatile functions of reflectarrays, steering reflected waves with polarization-dependent properties can find applications in areas such as signal transmission, polarization-sensitive measurements, and discrimination of incident polarizations. For example in the microwave regime, multilayer elements with rectangular patches [29] and cross-shaped microstrip loops [30] have been used as unit cells for constructing dual-polarization reflectarrays. Those realizations can achieve polarization-dependent beamforming functions, i.e., to scatter orthogonal polarization components into different directions. The scaled implementation of similar configurations with stacked multilayer structures in the terahertz and optical ranges is presently very challenging or even impossible to manufacture with the required precision.

In this work, a design of a polarizing beam splitter operating at 1 THz is proposed and experimentally validated. The device is based on the reflectarray concept and demonstrates the capability to separate the orthogonal polarization components of an incident beam and deflect

#211499 - $15.00 USD Received 8 May 2014; revised 15 Jun 2014; accepted 16 Jun 2014; published 23 Jun 2014

them into different directions. Two sets of orthogonally orientated dipole resonators arranged in interlaced triangular lattices are used for composing the unit cell, and the corresponding local reflection response is achieved by varying the length and width of the dipoles. A subarray is then constructed from the unit cells with the desired progressive phase distributions to respond to incident waves with polarization-dependent properties. By taking micro-fabrication tolerance into design consideration, the reflectarray is then fabricated for experimental validation. Both simulation and measurement are employed to verify the concept and assess the efficiency and polarization purity of the device.

2. Design and simulation

This section introduces the configuration of the reflectarray. The unit cell is described first, followed by the design of subarrays with the desired operation as a polarizing beam splitter.

2.1. The unit cell

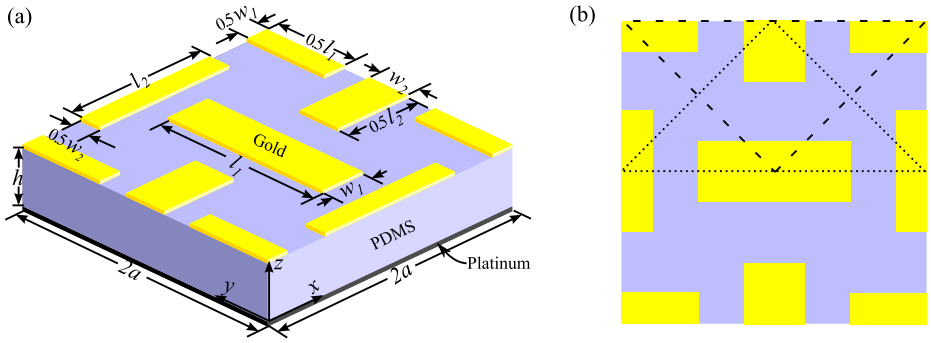

Fig. 1. Single unit cell of the proposed reflectarray. Each unit cell contains four dipoles with $a = 100\,\mu$m and $h = 20\,\mu$m. The lengths and widths of the dipoles are varied to obtain a nearly full cycle of phase response. (a) 3D view of the unit cell. (b) Top view of the unit cell indicating the interlaced triangular lattices.

Reflectarrays with polarization-dependent beam shaping ability can be in principle implemented using different approaches. For example, crossed dipoles with variable arm lengths [31, 32] or arrangements of orthogonal linear dipoles with variable dimensions [15, 30] can be employed. It was however observed that cross-talk between crossed dipoles in a non-uniform array can induce cross-polarized currents on the connected orthogonal arms, thereby degrading the polarization purity. Therefore, the approach considering interlaced arrays of orthogonal linear dipoles is preferred.

A unit cell for a uniform reflectarray is shown in Fig. 1. The structure is composed of two sets of orthogonal dipole resonators arranged in a compact layout, with each set corresponding to a particular polarization. The arrangement of the interlaced triangular-lattice is chosen for reducing the mutual coupling between the two sets of dipoles, while a compact layout significantly increases the efficiency of reflection compared to a loose arrangement of dipoles [33]. The unit cell is made of three layers: dipoles made of gold as the top layer, a polydimethylsiloxane (PDMS) dielectric spacer as the substrate and a platinum ground plane. The different metals provide etching selectivity during the micro-fabrication process, while PDMS exhibits acceptable loss in the terahertz range. The surface impedance model used in [23] is adopted for these metals with $Z_{\mathrm{Au}} = 0.287 + j\,0.335\ \Omega$ for gold and $Z_{\mathrm{Pt}} = 0.628 + j\,0.667\ \Omega$ for platinum, while the relative permittivity 2.35 and loss tangent 0.06 of PDMS are determined from

#211499 - $15.00 USD Received 8 May 2014; revised 15 Jun 2014; accepted 16 Jun 2014; published 23 Jun 2014

independent measurement. For operation at 1 THz, the size of the unit cell and the thickness of the PDMS substrate are selected at fixed values $2a = 200\,\mu\text{m}$ and $h = 20\,\mu\text{m}$, respectively. Different phase responses for a particular polarization can be achieved by varying the length and width of the active strip dipoles.

The phase response profile is simulated by using uniform infinite arrays in a commercial software package, Ansys HFSS, with periodic boundary conditions, and Floquet port excitation is applied. Based on numerical analysis, it is first confirmed that the effect of a dipole is negligible for the incident wave with polarization orthogonal to its axis. Therefore, in optimization of the unit cell shown in Fig. 1, the dipoles perpendicular to a given polarization are fixed at the dimension of $40\,\mu\text{m} \times 80\,\mu\text{m}$, while the length of the dipoles parallel to the polarization is varied from $40\,\mu\text{m}$ to $140\,\mu\text{m}$. In order to achieve a smoother phase curve with less stringent tolerances, a strategy based on variation of both length and width is found to be more efficient than variation of length only [28]. As shown in Fig. 2, narrower strip dipoles introduce a wider dynamic phase range but at the cost of a steeper phase change and reduced efficiency around resonance. In contrast, widening the dipoles decreases the dynamic range but smooths the transition of the phase curve around resonance. Based on this trade-off, we strategically adapt the dipole width for a wide enough dynamic range and relatively smooth phase change response for higher efficiency. We start the length variation with the shorter dipoles with a narrow width, to maximize the starting phase. With an increase in the dipole length, the width is linearly increased for a smoother phase response and low absorption around the resonance. After the resonance, the width of the dipoles is gradually decreased with further increasing length for a wider phase range. Away from resonance, the phase response is not sensitive to the width of the dipoles, and therefore a change in the width is not necessary. Based on these considerations, the length $l_{1,2}$ and width $w_{1,2}$ of the gold dipoles are varied according to the piecewise linear function relation:

$$w_{1,2} = \begin{cases} 32\,\mu\text{m} + 0.2\,l_{1,2} & \text{if } 40\,\mu\text{m} \le l_{1,2} \le 90\,\mu\text{m}, \\ 230\,\mu\text{m} - 2\,l_{1,2} & \text{if } 90\,\mu\text{m} \le l_{1,2} \le 105\,\mu\text{m}, \\ 20\,\mu\text{m} & \text{if } 105\,\mu\text{m} \le l_{1,2} \le 140\,\mu\text{m}. \end{cases} \tag{1}$$

These linear functions are illustrated as the solid line in Fig. 2.

The numerically resolved reflection phase and magnitude responses obtained as a function of the dipole length with the described width variation are given in Figs. 3(a) and 3(b), respectively. From the results, it is observed that a phase change of over 300° is achieved, while the highest loss on resonance is around 5.5 dB for a substrate loss tangent of 0.06. Since narrower strips have lower reflection efficiency on resonance (Fig. 2(b)), the maximum loss on resonance of the dipole is higher than the maximum loss of 1.2 dB observed in the square patch unit cell with similar material properties [23]. Nevertheless, considering that most dipoles in the reflectarray will be operating detuned from resonance, these results indicate that the proposed structure can offer a sufficient phase range for designing a reflectarray with reasonable reflection efficiency.

2.2. Subarray arrangement for terahertz beam splitting

The phase response data shown as blue solid line in Fig. 3(a) is applied for constructing subarrays composed of several unit cells. The full reflectarray will then consist of a periodic arrangement of such identical subarrays. In the present case, subarrays containing two orthogonal sets of dipoles, each composed of 6 elements are designed for deflecting a normally incident wave into two different directions. By following the design procedure of [23], at the operating frequency of 1 THz, i.e. $\lambda_0 = 300\,\mu\text{m}$ and $a = 100\,\mu\text{m}$, a progressive phase change of $\Delta\phi = \pm 60^\circ$

#211499 - $15.00 USD Received 8 May 2014; revised 15 Jun 2014; accepted 16 Jun 2014; published 23 Jun 2014

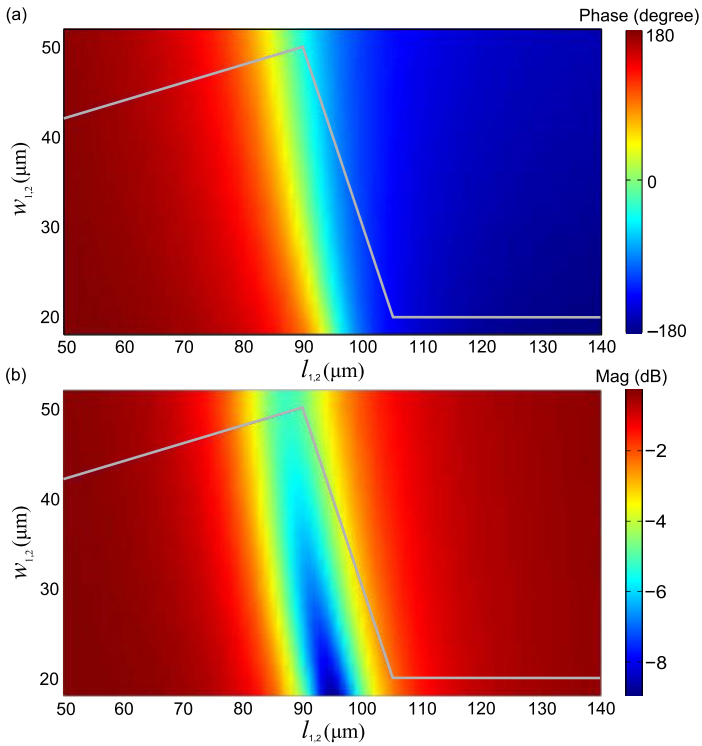

Fig. 2. Simulated reflection phase and magnitude responses as a function of the dipole length and width. The graphs show the strategy for determining the relation of the length and width of the dipoles to achieve a smooth and wide phase response with high efficiency. The lines correspond to the length and width relation given in Eq. 1.

between adjacent dipoles with the same orientation results in a beam deflection of

$$\theta = \arcsin \frac{\Delta\phi\lambda_0}{2\pi a} = \pm 30^\circ, \tag{2}$$

where θ is the deflection angle off the specular reflection in the incident plane.

The layout of the subarray obtained from this design procedure is shown in Fig. 4. By taking the fabrication tolerance into account, the length and the width of each dipole in the subarray are rounded to the next discrete value in micrometer. Due to different mutual coupling in the uniform and non-uniform arrays, the dimensions of the dipoles for constructing subarrays selected from the phase curve shown in Fig. 3(a) require fine tuning to achieve more accurate local phase response in the array. The corresponding optimized dimensions of the 12 dipoles are given in Table 1.

Instantaneous field distributions depicting the response of the reflectarray illuminated by a normally incident plane wave at 1 THz are shown in Fig. 5. The incident field is shown in Fig. 5(b) whereas the scattered fields for the TE and TM polarizations are demonstrated in Figs. 5(a) and 5(c), respectively. The scattered fields clearly illustrate that the normally incident plane wave is deflected into predefined directions according to the polarization. The relatively strong amplitude suggests good efficiency for the deflection. Due to the attenuation and the discrete resolution of the dipoles, the uniformity of the deflected wavefront is slightly degraded. This phenomenon is more obvious for the TE polarization than for the TM polarization. Similar observations have been reported in [23, 34], with a possible cause being the imbalanced

#211499 - $15.00 USD Received 8 May 2014; revised 15 Jun 2014; accepted 16 Jun 2014; published 23 Jun 2014

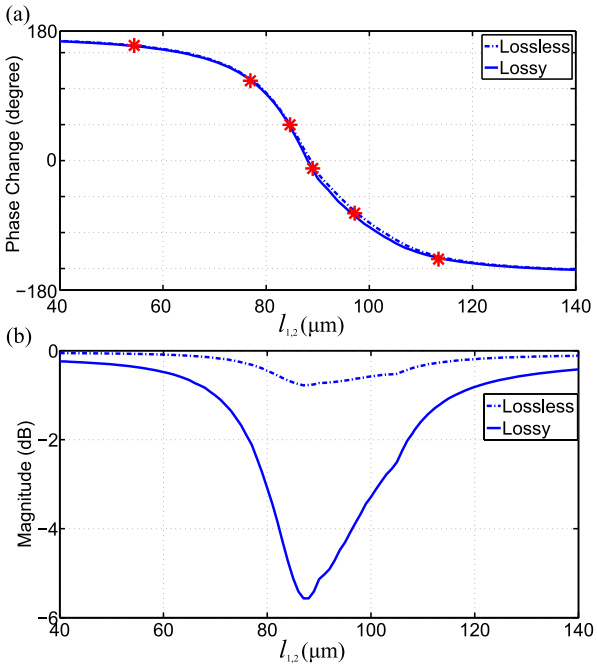

Fig. 3. Simulated complex reflection coefficients for uniform infinite dipole arrays. (a) Reflection phase response in degrees. (b) Reflection magnitude in dB at 1 THz as a function of the dipole size. The solid and dash lines are for configurations with the substrate loss tangent of 0 (lossless) and 0.06 (lossy), respectively. Six points on the phase curve with different widths and lengths indicate the required phase for constructing the beam-splitting reflectarray.

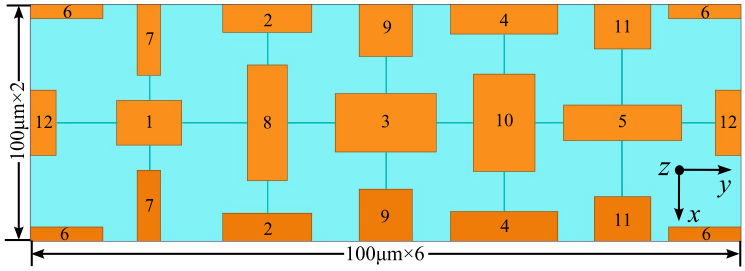

Fig. 4. Structure of one subarray made of 12 dipoles. The dimensions of the subarray are initially based on the phase response for a uniform array shown in Fig. 3. An iterative fine tuning of the dimensions is required to compensate for the variations of actual mutual coupling between dipoles in the non-uniform subarray.

response of each dipole in the TE polarization. It is noteworthy that, if the incident polarization is 45° in the *xy* plane, the normally incident beam will be split into two deflected beams of equal

#211499 - $15.00 USD Received 8 May 2014; revised 15 Jun 2014; accepted 16 Jun 2014; published 23 Jun 2014

Table 1. Dimensions of the dipoles for the optimized subarray. The units are in μm.

Dipole	1	2	3	4	5	6	7	8	9	10	11	12
Length	55	75	85	91	100	122	120	97	88	82	76	55
Width	38	48	49	50	30	24	20	34	45	52	48	43

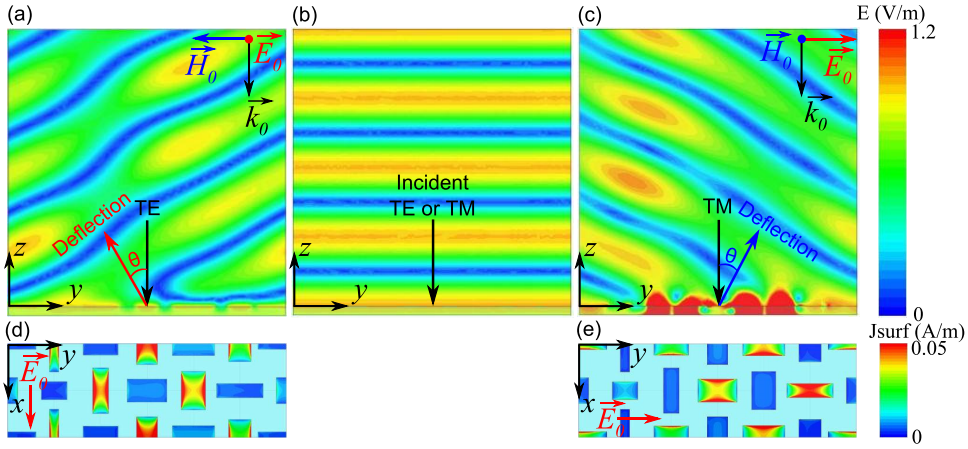

Fig. 5. Instantaneous incident and scattered field distributions from the reflectarray in TE and TM polarizations at 1 THz. When the incident wave (b) is impinging normally to the surface of the reflectarray, the TE and TM polarized wave are deflected into two different directions with the angles of -30° and $+30^\circ$ as shown in (a) and (c), respectively. The corresponding magnitude of the surface current density on the dipoles is shown in (d) and (e).

power with the sign of the deflection angle being determined according to the linear polarization component. The magnitudes of the surface current density plotted in Figs. 5(d) and 5(e) confirm that the two sets of dipoles are selectively excited by the corresponding polarization.

3. Reflectarray fabrication

In order to validate the reflectarray designed for beam splitting, we fabricate a reflectarray that contains a periodic arrangement of 252×84 subarrays shown in Fig. 4. This corresponds to a total sample size of 50.4 mm $\times$ 50.4 mm, which fits a standard 3 inch wafer and is sufficient to cover a collimated beam in the measurement. The details of the fabrication process and sample are given in this section.

A 3 inch silicon (100) oriented wafer was cleaned with solvents, dried with high purity compressed nitrogen, and coated with the metallic ground plane. The ground plane was composed of a 200 nm platinum thin film, with a 20 nm titanium thin film utilized to promote adhesion to silicon, deposited at room temperature by electron beam evaporation. A two-part, high purity, silicone elastomer — PDMS — was prepared as a mixture of curing agent and pre-polymer in a 1:10 weight ratio [35, 36]. This PDMS is used to define the controlled thickness dielectric layer of 20 μm in the reflectarray. To attain 20 μm, the polymer is spin-coated at 1,950 rpm, with an acceleration of 1,000 rpm/s^2 for a 30 s duration. The layer is then cured at 72°C for 1 h. The attained thickness was verified experimentally by surface profilometry. The metallic dipoles

#211499 - $15.00 USD Received 8 May 2014; revised 15 Jun 2014; accepted 16 Jun 2014; published 23 Jun 2014

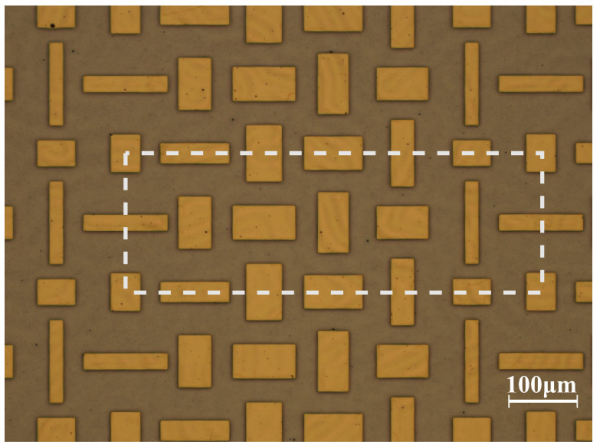

Fig. 6. Optical micrograph of a small part of the reflectarray. The dashed rectangle encloses one of the subarrays.

were defined using 200 nm thick gold films, with a 20 nm thick adhesion layer of chromium. This metallic bilayer is patterned using photolithography and wet etching, with the choice of platinum for the ground plane ensuring selectivity. The residual photoresist is cleaned with solvents, in preparation for terahertz measurements. A micrograph of a small region of the final sample is shown in Fig. 6, with one subarray highlighted.

4. Results and discussion

The sample has been measured using a commercial terahertz time-domain spectroscopy (THz-TDS) measurement system, namely, Tera K15 developed by Menlo Systems GmbH. The measurement setup and experimental results are given in this section.

4.1. Measurement system

A photograph of the measurement setup is shown in Fig. 7(a) with a corresponding schematic representation in Fig. 7(b). The two identical lenses with an effective focal length of 54 mm are used for obtaining a collimated beam. The emitter and lens #1 are mounted on a fixed rail. The sample is mounted on a platform with angular scale that can be rotated for adjustment of the incidence angle. Particular care is necessary to ensure that the surface of the sample has its center located on the rotation axis. A femtosecond optical pulse from a near-infrared laser source is guided by a fiber to the terahertz emitter. The generated broadband terahertz radiation guided from the emitter is collimated by lens #1 before impinging the reflectarray. The detection part of the system comprises lens #2 that focuses the scattered fields onto the detector. Both of the components are mounted on a rotation arm pivoting around the sample center point. This arrangement allows convenient scanning the radiation pattern in a wide angular range. For the reference, a gold-coated mirror replaces the reflectarray, and the incident and reflected angles are set to 15°. For each polarization, two measurements are carried out on the sample. Firstly, the incidence angle is set to 15° for measuring the specular reflection off the reflectarray sample. Secondly, the sample is illuminated at normal incidence in a given polarization, while the detection arm is rotated to scan the scattered terahertz waves at different angles. In the measurement of the radiation patterns, the scanning ranges for both the TE and TM polarizations are limited to the ranges, $-48°$ to $-22°$ and $22°$ to $48°$, because the minimum clearance between

#211499 - $15.00 USD Received 8 May 2014; revised 15 Jun 2014; accepted 16 Jun 2014; published 23 Jun 2014

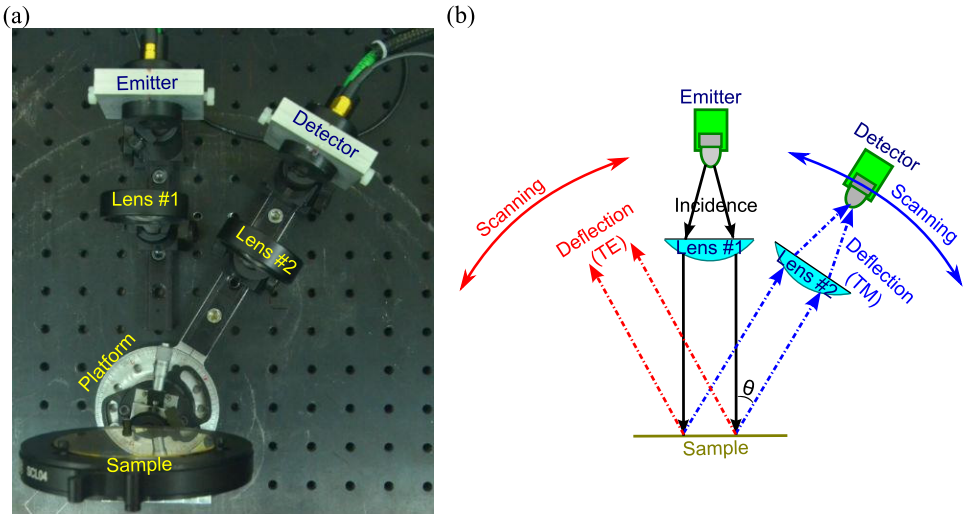

Fig. 7. Measurement system. (a) Photograph of the measurement system. (b) Corresponding schematic. The beam from the emitter is collimated by lens #1, and incident on the surface of the sample. Lens #2 collects and focuses the scattered wave onto the detector. Lens #2 and the detector are fixed on a rotating arm pivoting around the location of the sample center. This arrangement allows a wide angular range to be scanned.

the lens #1 and lens #2 precludes measurements around the specular direction. Measurements are not carried out beyond 48° or -48° because the deflection becomes negligible. A measurement angular resolution of 0.5° is sufficient for resolving the main features of the deflected beams. For measurements in the other polarization, both the emitter and detector are rotated by 90°, and the measurement procedure is repeated. All the measurements of the reflectarray are normalized using the mirror reference to remove any system dependency.

4.2. Measurement results

For the TE polarized incident wave, the normalized spectra for specular reflection and -30° deflection are shown in Fig. 8(a). A distinct notch at around 1 THz can be observed from the sample specular reflection. This is because considerable energy around this frequency is deflected away from the specular direction. At the predesigned deflection direction of -30°, the strong deflection peak appears close to the design frequency of 1 THz as shown in Fig. 8(a) with the red solid line. It is observed that, for the TE polarized incident wave, 75% of the incident magnitude is deflected into the designed direction. Similar results are obtained for the TM polarization, however with the difference that the deflection direction is on the other side of the incident direction. The corresponding measured results are given in Fig. 8(b). Strong deflection can be observed at around 1 THz in the designed deflection of $+30^\circ$ with a deflection magnitude of around 80%, thus showing slightly higher deflection efficiency compared to the TE polarization.

In order to characterize the angular behavior of the deflected beams for normal incidence, the radiation patterns of the reflectarray for both of the TE and TM polarizations are simulated and measured as shown in Fig. 9. In the HFSS simulations, the radiation pattern of the TE and TM polarizations can be numerically obtained using an approach based on the array factor, but neglecting edge effects. The results shown in Figs. 9(a) and 9(b) demonstrate the predicted polarization-dependent deflections. A specular reflection component, i.e. a feed im-

#211499 - $15.00 USD Received 8 May 2014; revised 15 Jun 2014; accepted 16 Jun 2014; published 23 Jun 2014

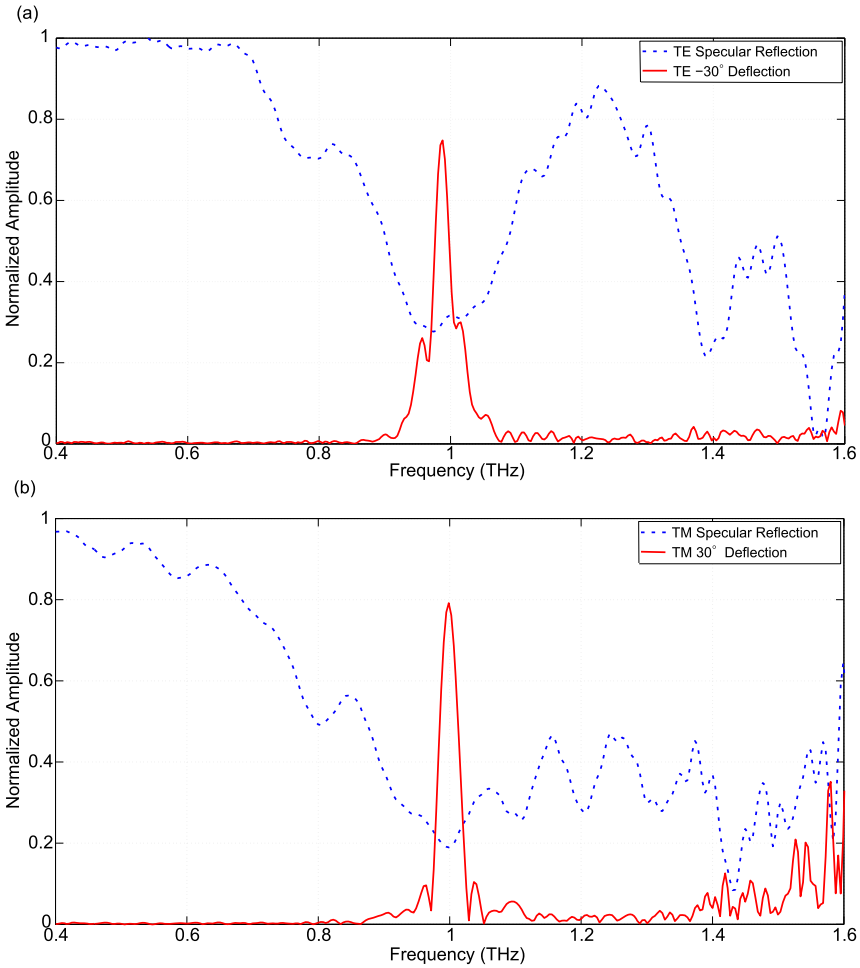

Fig. 8. Measured normalized amplitude spectra for specular reflection (blue dashed line) and deflection (red solid line). The 15° incident waves with TE (a) and TM (b) polarizations are specularly reflected and distinct notches at around 1 THz are observed in the spectra, whereas the normally incident TE and TM waves are efficiently deflected into $-30°$ and $+30°$, respectively.

age lobe [37], exists but is around 10 dB lower than the maximum deflection. This specular component can also be interpreted as imperfectly suppressed zeroth-order spatial harmonics associated with the subarray periodicity. The measured radiation patterns at 1 THz are given in Figs. 9(c) and 9(d) for the TE (red line) and TM (blue line) polarizations, respectively. Because of different excitations, plane waves for simulations and Gaussian beams for measurements, wider deflection beams and lower side lobes are observed in measured radiation patterns when compared with the simulated patterns. The measured cross-polarized components caused by grating lobes in the deflected beams are -27 dB for the TE polarization and -29 dB for the TM polarization. However, it is noted that those values are most likely limited by the measurement system dynamic range.

As for the spectral characteristics of the reflectarray, the normalized scattered wave amplitude is shown in Fig. 10. The magnitude is plotted in linear scale as a function of frequency and scan

#211499 - $15.00 USD Received 8 May 2014; revised 15 Jun 2014; accepted 16 Jun 2014; published 23 Jun 2014

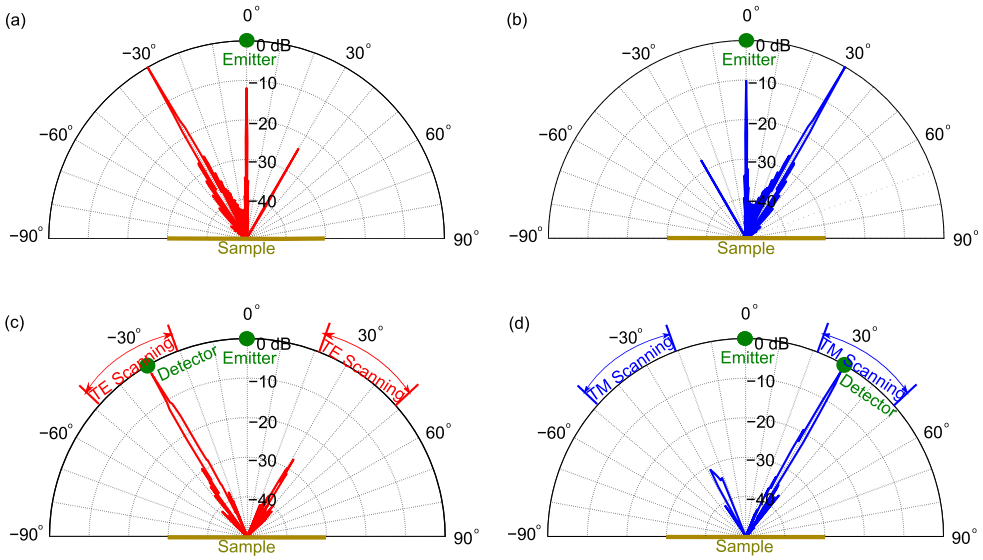

Fig. 9. Radiation patterns at 1 THz for TE and TM polarized incident waves on a logarithmic scale. The normally incident wave with the TE or TM polarization can be efficiently deflected into the direction of -30° or $+30^\circ$. (a) and (b) Simulated radiation patterns for the TE and TM polarized incident plane wave, respectively. (c) and (d) Measured results for the TE and TM polarized incident Gaussian beam, respectively.

angle. It is again demonstrated that the strongest deflection take places around the specified frequency in the designed directions for both of the TE and TM polarizations. Off the optimum, the deflection efficiency degrades gradually. Away from the predesigned main lobes for both the TE and TM polarizations, grating lobes introduced by the periodic configuration in subarrays are apparent in Fig. 10 beyond 1.4 THz.

The above measurement results demonstrate promising prospects for the designed reflectarray for terahertz beam splitting. However, there are two aspects that could be improved for further enhancing the performance of the reflectarray. Firstly, the angle for the maximum deflection amplitude of the TE and TM polarized incident waves shifts from the designed $\mp 30^\circ$ at 1 THz to measured -28° at 1.04 THz and $+29^\circ$ at 1.03 THz, respectively. This slight disparity is caused by fabrication tolerance. In particular, the substrate thickness of the fabricated sample has been estimated to be 17 μm, rather than the target thickness of 20 μm. The fabrication tolerance moves the frequency for the maximum deflection slightly off the designed optimal frequency, which translates in a shift of the angle for the maximum deflections, i.e. through the phenomenon of beam squint with frequency [38]. Secondly, the deflection efficiency for the TE and TM polarizations could be improved by using dielectric substrates with lower loss tangent.

5. Conclusion

A terahertz reflectarray with orthogonal strip dipoles in an interlaced triangular-lattice configuration has been proposed and designed for operation as polarization beam splitter. The performance of the fabricated prototype has been measured with a THz-TDS system. Both the simulation and measurement results successfully verify that the designed reflectarray can efficiently deflect the incident waves into different directions depending on the incident linear polarization with an efficiency of over 60% and polarization purity of at least -27 dB. For higher

#211499 - $15.00 USD Received 8 May 2014; revised 15 Jun 2014; accepted 16 Jun 2014; published 23 Jun 2014

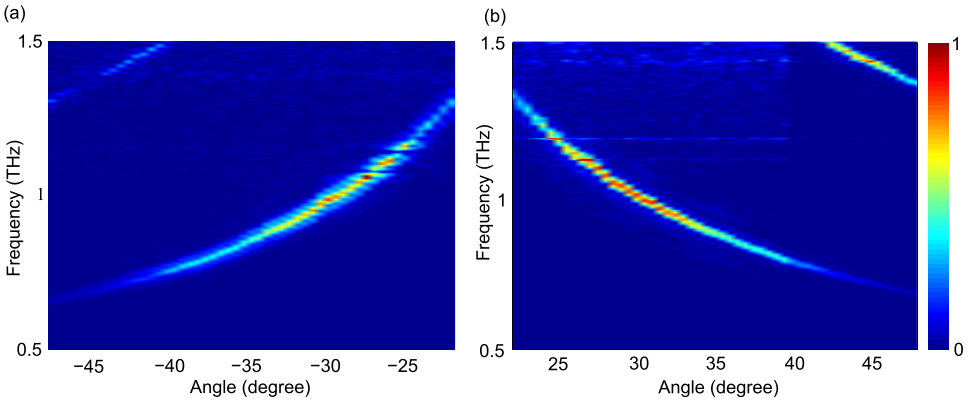

Fig. 10. The normalized deflection magnitudes in linear scale as a function of the frequency and scan angle for TE (a) and TM (b) polarizations.

deflection efficiency, a lower loss material could be applied as the substrate. As the reflectarray construction is based on resonant elements, the -3 dB bandwidth of the designed beam splitter is limited at about 3% in the present case. The limited bandwidth behaviour of the terahertz beam splitter could be improved by considering multi-layer approaches developed in the microwave regime [39]. The challenging adaption of these techniques to the terahertz regime will be the topic of future investigations. These reflectarrays could be applied as optical components for polarization discrimination or as polarization demultiplexers for terahertz communications.

Acknowledgments

Tiaoming Niu acknowledges support from the Fundamental Research Funds for the Central Universities (No. LZUJBKY-2014-43). Madhu Bhaskaran and Sharath Sriram acknowledge ARC Australian Post-Doctoral Fellowships via Discovery Projects DP1092717 and DP110100262, respectively. Sharath Sriram acknowledges partial support from Victoria and AFAS-Vic Fellowships. Derek Abbott and Christophe Fumeaux acknowledge the ARC Future Fellowship funding scheme under FT120100351 and FT100100585, respectively.